World Conference on Timber Engineering Oslo 2023

MOISTURE PREDICTION OF TIMBER FOR DURABILITY APPLICATIONS USING DATA-DRIVEN MODELLING

Seyyed Hasan Hosseini[1], Jonas Niklewski[2], Philip Bester van Niekerk[3]

ABSTRACT: Durability and service life assessment is a major challenge for the design and use of timber in outdoor weather exposed environments. Rate of deterioration by fungal decay is closely linked to variations in wood moisture content. The objective of the present paper is to test and evaluate different data-driven models based on the multilinear regression (MLR) and artificial neural network (ANN) approach. Moisture content was predicted at the surface and core of a rain-exposed wooden element in the context of durability and service life assessment. Synthetic data stemming from a numerical model were used to fit time-series weather variables, including different combinations of time-lagged daily precipitation, relative humidity, and temperature, to temporal variations of daily average wood moisture content. Based on a set of statistical and qualitative analyses, using the weather variables lagged by 0 – 11 days as input variables for 11 mm depth moisture prediction, ANN showed the highest accuracy and least sensitivity to its initial setups, and could significantly outperform the MLR with the same input variables. The resulting models for surface and core moisture prediction were then tested against two different datasets consisting of measured data from wood specimens subjected to outdoor exposure.

KEYWORDS: Moisture content, Durability, Model, Artificial Neural Network (ANN), Regression

1 INTRODUCTION

Service life assessment is a major concern for timber in weather exposed environments. The problem largely stems from the natural deterioration caused by fungal decay, a mechanism that is exacerbated by poor moisture management and suboptimal use of materials. Recent efforts to systemise service life assessment of timber have resulted in various performance-based design guidelines for European conditions. The guideline in [1] is based on a dose-response relationship where the rate of fungal decay is expressed as a function of wood moisture content and temperature. Therefore, dose-response models enable service life assessment based on wood moisture content and temperature [2].

Wood moisture content is a measure of the material microclimate and one of the main vectors for biotic deterioration by fungal decay. In general, the moisture variation of wood depends on various factors such as local weather, the wooden element's distance to ground, and detailing. Brischke et al. [3] categorize these influences as 'indirect', since they are primarily linked to service life via their effect on moisture content. For modelling purposes, moisture content can either be obtained by measurement [4] or modelling [5,6].

Using a modelling approach, the wood moisture content is estimated based on these indirect factors and in a subsequent step, used with dose-response models to predict service life. Figure 1 shows how indirect variables (weather) can be used via numerical modelling to estimate direct variables (moisture content), which can then be used via empirical damage functions to model wood decay. The limit state defines the acceptable response in terms of material deterioration and the service life is defined as the period until the limit state is reached.

Numerical modelling of moisture transport in wood is an integral part of several branches of wood technology. Common applications include the migration of free water from green lumber during drying [7] and moisture gradients of sheltered structural timber during service [8]. These models transfer poorly to predictions of service life where the wood surface is subject to cycles of wetting and drying and the main region of interest lies above cell wall saturation. The simple numerical model developed in [6] was made specifically for use with dose-response models and integration with performance-based service life design.

The integration of numerical moisture modelling in service life prediction led to improved accuracy, but simultaneously introduced a dependency on commercial software and increased the computational time. These

[1] Seyyed Hasan Hosseini, Lund University, Department of Building and Environmental Technology, Sweden, hasan.hosseini@tvrl.lth.se
[2] Jonas Niklewski, Lund University, Department of Building and Environmental Technology, Sweden, jonas.niklewski@kstr.lth.se
[3] Philip Bester van Niekerk, University of Goettingen, Wood Biology and Wood Products, Germany, philipbester.niekerk@uni-goettingen.de

https://doi.org/10.52202/069179-0495

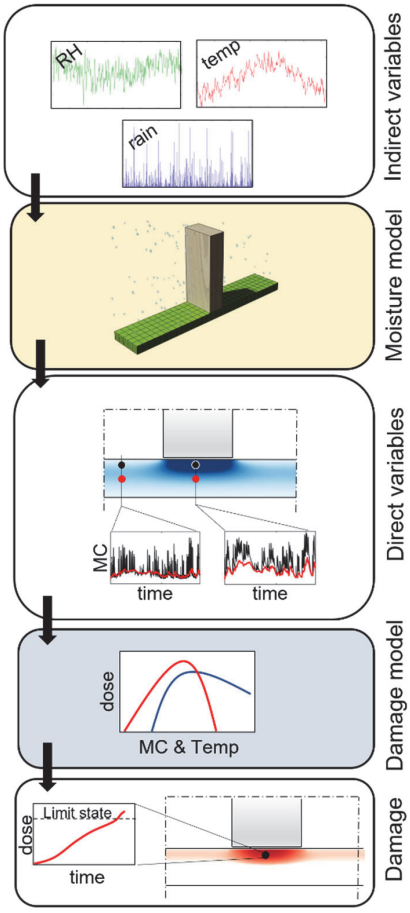

Figure 1: *Framework to predict moisture content and damage from environmental variables.*

downsides limit the practicality of numerical modelling. Alternatively, data-driven (DD) models that are considerably less computationally expensive than numerical models can easily be integrated into digital design tools for applications of service life prediction.

This paper explores new DD approaches for moisture content prediction of rain-exposed wood. The aim is to develop an efficient alternative to existing numerical models for moisture content prediction, with minimal loss in accuracy. For this purpose, synthetic data obtained from the numerical model in [9] were used for model development. A set of DD models based on the multiple linear regression (MLR) and artificial neural network (ANN) approaches, under various settings and input variable assumptions, were developed and evaluated via statistical and qualitative methods. The models are then tested against two different data sets based on real measurements.

2 METHOD

2.1 Data

2.1.1 Synthetic data for model development

Each data set (synthetic or measured) includes time-series of the moisture content at a specific depth from the wood surface (response/output variable) and relative humidity, precipitation, and temperature (predictor/input variables). A model was first fitted and verified against a set of synthetic data obtained from a one-dimensional numerical model for moisture transport in Norway spruce (*Picea abies*) wood [3]. The model geometry was modelled as 22 mm, reflecting the thickness, and transport properties reflecting moisture flux perpendicular to the grain direction. More details regarding the dataset can be found in [10], where the same data was used to map the decay hazard in a variety of different climates.

2.1.2 Measured data for testing

Two different datasets were used for testing the model against real measurements of varying moisture content. Both datasets consisted of measurements of moisture content obtained for Norway spruce boards in outdoor conditions, with weather data recorded in parallel. Moisture content was measured by resistance-type moisture sensors using insulated electrodes in both cases. Important to note is that the valid range of resistance-type measurements is (generally) below the point of cell wall saturation.

The first data set came from [11] and spanned a period of about 2.5 years. Measurements of moisture content were obtained from horizontal boards with a thickness of 22 mm. The top face was exposed to precipitation while the bottom face was considered sheltered and end-grain surfaces were sealed by silicone-based adhesive. Measurements were obtained at a depth of 11 mm from the top face, i.e., at half of the board's thickness. The geometry and exposure setup of the dataset were consistent with the numerical simulations used for DD modelling.

The second dataset came from [12] and spanned a period of about two years. Measurements of moisture content were obtained from inclined (45º) boards with a thickness of 20 mm. The test included specimens with both planed and pre-weathered top faces. Here, only the measurements obtained from pre-weathered samples were used. All short sides as well as the back face of the boards were sealed by silicone-adhesive, leaving only the top face exposed to the ambient weather. Surface moisture content was monitored every 5 minutes. After 18 months of exposure, the test setup was sheltered from precipitation, but remained outdoors for an additional 6 months. The specimens were similar to the geometry used for producing the synthetic data, but it should be noted that the specimen thickness was 2 mm less, the backside was sealed, and the boards were inclined. However, the small discrepancy in thickness nor the sealed bottom face were expected to have a significant influence on the surface moisture content of the exposed face.

https://doi.org/10.52202/069179-0495

2.2 MODELLING

The study includes several approaches for DD moisture prediction of rain-exposed wood, preliminary based on MLR and ANN approaches with various assumptions of input variables. The simplest MLR model can be defined as:

$$u_t = \beta_0 + \beta_1 \times RH_t + \beta_2 \times T_t + \beta_3 \times p_t \qquad (1)$$

where t is the index of time, and β_0, β_1, β_2, and β_3 are constants relating the relative humidity RH, temperature T, and precipitation p to the moisture content u at a given depth of a horizontal wood specimen (e.g., 11 mm). The reference values for u were outputs of a numerical model developed based on an average year of exposure for different climate data of about 550 sites across Europe [10]. More complex MLR could be achieved by relating u_t to RH, T, and p from t, t-1, t-2, …, t-L where L is a maximum time lag to consider potential contributions from previous time steps. The constants, as expected from eq. 1 (β_0, …, $\beta_{(L+1)\times 3}$), were obtained using the conventional least square method for a set of known u (synthetic data by numerical model). A suitable range of L was primarily estimated by cross-correlation analysis, which evaluates linear relationship between u and time-lagged versions of p, T, and RH. Then, L was fixed after evaluating the performance of ANN with multiple options from the estimated range, to take the non-linear relationships into account. These analyses were done for the 11 mm depth moisture content, but the resultant L was assumed valid for shallower depths too.

While the input variables used for MLR and ANN could be the same, the way they were related to moisture content was different. The equations used for ANN, are usually better described using an architecture resembling the neural network of a human brain, as exemplified in Figure 2.

For the example of Figure 2, each black node on the input layer includes a data vector corresponding to an average daily value of an input variable (e.g., RH). Then, each red neuron on the first hidden layer (HL) multiplied the input variables by a corresponding scalar weight w and added a scalar bias b to the sum of all weighted input variables. Finally, a transfer function (f) was applied to give a value n to the neuron. Thus, the mathematical expression for a neuron on the first HL (h=1) can be written as:

$$n_{j,h=1} = f\left(\sum_{i=1}^{4}(X_i \times w_{i,j,h=1}) + b_{j,h=1}\right) \qquad (2)$$

where j is the index of neuron (j=1, …, 5 for h=1). Generally, a neuron on the second HL considers the results of the neurons on the first HL as input variables, and so forth for the next HL and output layer. To calibrate the parameters of ANN (w and b), an iterative optimization problem was solved to minimize the mean squared error (MSE) between the estimated and reference moisture u. The process starts with random initial parameters (variable between -1 and 1, similar range as the normalized input variables), which were changed at multiple iterations until a minimum MSE was achieved.

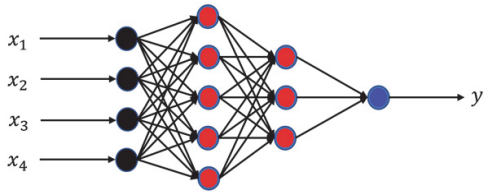

Figure 2: *A feedforward ANN architecture, connecting input variables X1-X4 to output variable y through two hidden layers (HLs) with five and three neurons (red) between input layer (black) and output layer (blue).*

Then, f had a mathematical form, making MSE differentiable with respect to the parameters w and b. In this study, $f(n)=n$ for the output layer, and $f(n)=(\exp(2\times n)-1) / (\exp(2\times n)+1)$ for the HLs as a conventional method. The suitable ANN architecture is usually a trial-and-error problem, and this study used up to two HLs and 4–20 neurons per HL.

Conventional ANNs are usually prone to overfitting due to the use of many parameters (i.e., perfect fit to the calibration data, but noisy for new data). To prevent this, a stopping rule was defined based on a part of the data (validation portion) separate to the data used for direct calibration of the ANN (training portion). This study used a so-called, "maximum validation fail (MVF)" criterion, which monitors validation MSE at the iterations. This criterion stops modelling when the MSE in the validation dataset increases for 10 consecutive iterations regardless of possible improvement in training for additional iterations. As a result, the parameterization is fixed based on the iteration that resulted in minimum validation dataset MSE (rather than training dataset MSE). The length of the study's dataset was near two hundred thousand, i.e., number of sites × (365 – L) days, due to the use of time-lagged inputs, which was quite long compared to the number of ANN parameters. So, overfitting could be less problematic. However, the MVF criterion was still useful to address the possible issue of ANN converging at a local minimum. To clarify, it is favourable to stop an ANN parameterization based on the MVF criterion and repeat it with new random initial parameters that are likely to end at a new final parameterization and exit the local minima. Finally, the ANN with minimum validation MSE among all repeats was selected. Alternatively, a hybrid of outputs from a few top ranked ANNs by validation MSE could be used, which was shown useful for generalization of the ANN outputs for other DD problems (see e.g. [13]).

As said at the beginning of this section, different models were developed based on various assumptions of input variables. These assumptions were different in, firstly, the number of lags used to consider effects of previous weather conditions, and secondly, the definition and number of principle components of the time-lagged input variables used based on the PCA method [14]. Thus, while L increased the number of input variables, PCA was a method to combine and reduce them. Thus, 12 different input variable combinations were defined as follows.

- **Direct_inputs**, where all the time-lagged versions of the three weather variables (lags 0, 1, …, L days) were directly used (without any reduction via PCA). So, in total, there were 3×(L+1) input variables.
- **All_PCA5**, **All_PCA6**, **All_PCA7**, **All_PCA8**, and **All_PCA9**, where all variables in **Direct_inputs** were reduced, in total, to 5, 6, 7, 8, and 9 variables, respectively, via PCA.
- **Lags_PCA3**, **Lags_PCA4**, **Lags_PCA5**, and **Lags_PCA6**, where, for each of the three weather variables, the L+1 time lagged versions were reduced to 3, 4, 5, and 6 variables; so, in total, there were 9 (=3×3), 12 (=3×4), 15 (=3×5), and 18 (=3×6) input variables, respectively.
- **Variables_PCA1**, and **Variables_PCA2**, where, for each of 0, 1, …, L lags, the three weather variables were reduced to 1, and 2 variables; so, in total, there were (L+1), and (L+1)×2 input variables, respectively.

The developed ANNs based on the above combinations of input variables were evaluated for a verification portion (Figure 3), separated entirely from the training and validation portions, using the modelling performance criteria Nash-Sutcliffe Efficiency (NSE) that is:

$$NSE = 1 - \sum \frac{(\hat{u}_i - u_i)^2}{(u_i - \mu)^2} \qquad (3)$$

where, $\hat{u}$ and u stand for estimated and reference moisture content, μ is average of u, and i denotes the index of the verification data. NSE can be reformulated as NSE=A–B–C; where A=2 × $\frac{\hat{\sigma}}{\sigma}$ × ρ, B=$(\frac{\hat{\sigma}}{\sigma})^2$, C=$(\frac{\hat{\mu}-\mu}{\sigma})^2$, $\hat{\mu}$ and $\hat{\sigma}$ are mean and standard deviation of $\hat{u}$, ρ is correlation coefficient (perfect linear relationship between $\hat{u}$ and u is ρ=1, while the lack of linear correlation is ρ=0), and σ is standard deviation of u. Hence, NSE is different from the coefficient of determination (R^2=ρ^2), in that it includes additional elements considering the biases in estimates of variance (in B) and mean (in C), along with ρ (in A) to describe the modelling performance. The perfect accuracy is NSE=1 while NSE<0 is a condition worse than the use of μ as a simple estimator. NSE is widely used as an independently interpretable performance index of DD predictive modelling relying on weather data in various fields (e.g., [15,16]).

It is noted that, for a fair distribution of variable moisture data, in all portions in Figure 3, the Scheffer climate index, SCI, as described in [17], was calculated for the studied sites to classify them into 40 classes, with a frequency of 13 to 14 sites per SCI class, equivalent to 0–2.5, 2.5–5, …, 95–97.5, 97.5–100 percentiles of SCI as shown in Figure 4. Then, from each class, one site was randomly selected for "verification", another for "validation", and the remaining 11-12 for "train".

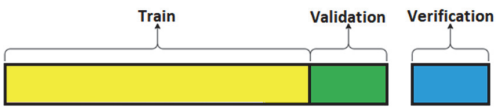

Figure 3: *Splitting of the data length into portions.*

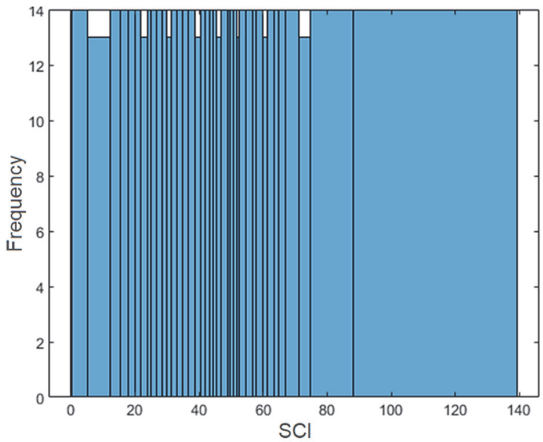

Figure 4: *Classification of the sites into 40 classes of SCI.*

3 RESULTS AND DISCUSSION

3.1 Model performance against synthetic data

To predict daily wood moisture content via ANN and MLR, L was defined first. Based on the cross-correlation analysis in Figure 5, among all weather variables, the highest correlation (ρ~0.55) was observed for RH at L=2; meaning that u had the highest linear relationship to relative humidity of two days earlier. For RH, ρ remains above 0.4 for up to L=10 and gradually decreases with further increases of L. Negative ρ for T indicates reverse changes of u and temperature. Among the variables, the absolute value of ρ dropped the fastest (slowest) for precipitation (temperature) from the max ρ at L=2 to the more stabilized ρ at higher L. Generally, a suitable range of options for L was estimated not to exceed 6 – 13 days, when ρ stabilized for different variables. Therefore, the development of ANNs using the 12 input variable combinations (as defined in section 2.2) was repeated for each choice of L between 6 – 13. The NSE of the ANNs are summarized in Figure 6a (for L=6–9) and Figure 6b (for L=10–13).

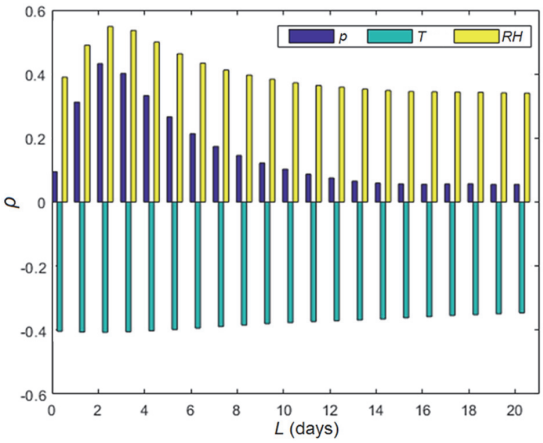

Figure 5: *Cross-correlation between 11 mm depth synthetic moisture content and three weather variables lagged by 0 – 20 days.*

https://doi.org/10.52202/069179-0495

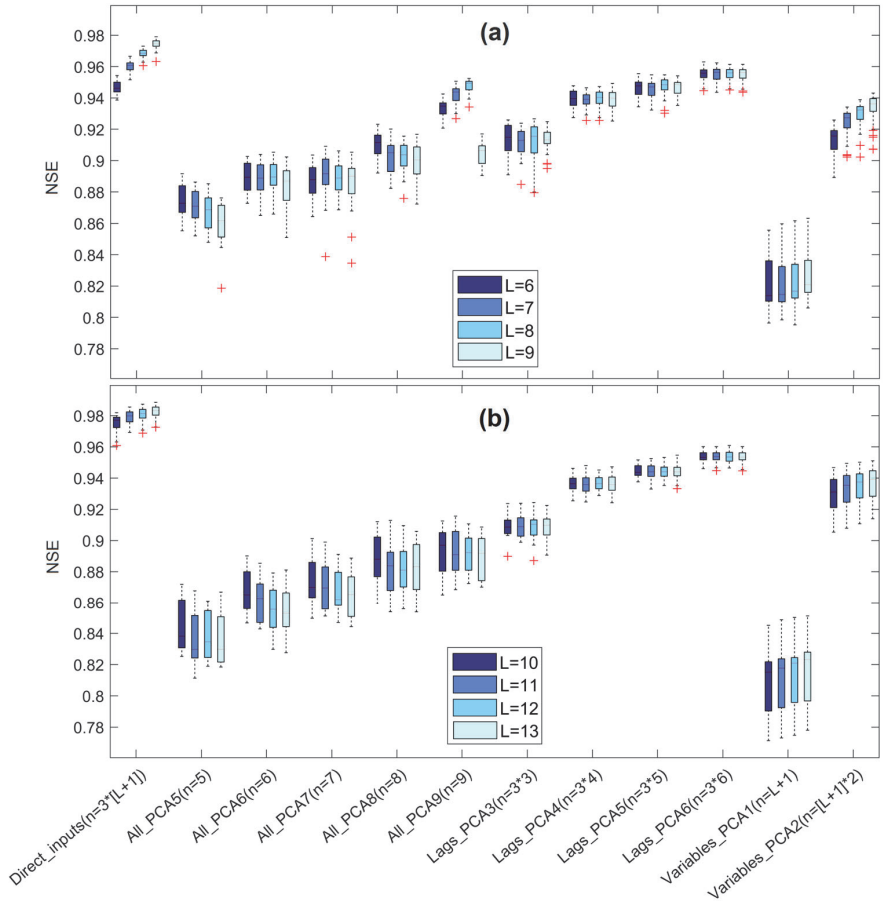

Figure 6: *Boxplots representing the range of NSE obtained from up to 25 repeats of ANNs developed for 11-mm depth moisture content modelling using time-lagged input variable combinations. On the horizontal axis,* n *gives the total number of input variables based on (a) L=6–9 days and (b) L=10–13 days. Red plus markers show outliers.*

The type of delayed response seen in Figure 5 and discussed in the previous paragraph is typical for moisture transport phenomenon. The delay primarily depends on the transport properties and depth. The increase in moisture content stemming specifically from lagged precipitation tends to decrease with decreasing distance to the rain-exposed surface. Therefore, less lags could be used for predicting the response at 1 mm (e.g., compared to 11 mm) depth. As mentioned earlier, the lags were, however, not varied between the two depths.

In Figure 6, for every input variable combination (e.g., Direct_inputs), eight boxplots are presented, corresponding to different choices of *L*. Each boxplot shows the range of obtained NSE for the repeats, where the bottom and top of each box corresponds to the first and third quartiles (q_1 and q_3, respectively), and the line within the box depicts the median NSE. The whiskers extend to the most extreme NSE, with outliers shown by the '+' marker. Outliers were greater than $q_3+w\times(q_3-q_1)$ or less than $q_1-w\times(q_3-q_1)$, where w was 2.7×(standard deviation of NSE). All the outliers in Figure 6 are located below the boxes (least NSE), which could mean that the outliers belonged to the repeats where ANN was trapped within the local minima of MSE.

As a result, while higher NSE is favourable, smaller intervals between the q_3 and q_1 (i.e., shorter boxes), show less sensitivity of modelling to the employed ANN architecture and initial random parameters in repeats. The shortest boxes were primarily observed for the ANN models using Direct_inputs, and Lags_PCAx (when x=6, 5, or 4). However, Direct_inputs resulted in the highest NSE that increased with increases of *L*, e.g., from 6 to 9 days (Figure 6a). Further increases of *L*, e.g., from 10 or 11 to 13 days (Figure 6b), did not result in a significant NSE increase for Direct_inputs. Lags_PCAx generally showed sensitivity to x rather than *L*.

Thus, the accuracy of predictions using input variable combinations of the form Lags_PCAx was mainly controlled by the adopted number of principal components, e.g., see the jumps in NSE values from Lags_PCA3 to Lags_PCA4 (Figure 6).

In view of the above, Direct_inputs and *L*=10 or 11 days seem to be enough for accurate prediction of the synthetic wood moisture content with a minimum sensitivity to ANN architecture and initial random parameters. Using such a combination for input variables, ANN could significantly outperform MLR. For example, by *L*=10, the

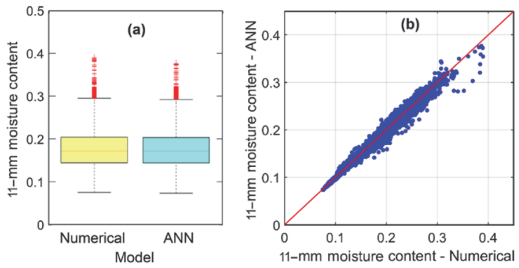

Figure 7: *Comparison of synthetic vs modelled (ANN) 11-mm moisture data in box plot (a) and scatter plot (b)*

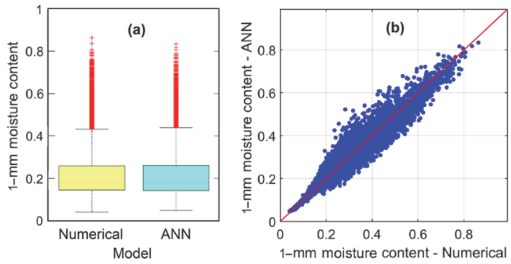

Figure 8*: Comparison of synthetic vs modelled (ANN) 1-mm moisture data in box plot (a) and scatter plot (b).*

corresponding NSE for MLR was 0.86, so 10% smaller than the least (outlier) NSE shown in Figure 6b for ANN under Direct_inputs and L=10 (0.96). Also, for an arbitrary ANN (not the best) with the same inputs, mean absolute error in verification of ANN was three times smaller than that of MLR (0.004 vs 0.013).

So far, the evaluations are based on the statistical performance criteria of the DD moisture content prediction at 11-mm depth. Figures 7 and 8 help to visually examine the predicted moisture content by ANN versus the synthetic moisture content by numerical model (as reference) at 11- and 1-mm depth, respectively. The box plots (Figures 7a and 8a) compare the synthetic and modelled data variability while the scatter plots (Figures 7b and 8b) compare the exact data points with the 45-degree line equivalent to the best fit for verification. Based on Figure 7a, except for a few top outliers ("+" markers), the elements of the boxplots for ANN and synthetic data match together, which is supported by the scatter plot (Figure 7b) showing a generally good agreement between ANN and synthetic data except for a few data points of synthetic values above 0.3 that are underestimated by ANN. Similarly favourable results can be observed for 1-mm moisture prediction in Figure 8. However, as seen in Figure 8b, the extreme data points (e.g., synthetic data below 0.2 and above 0.6) do not show significant over- or underestimations by ANN, and the highest discrepancies were observed for data points between 0.2 and 0.4.

Further evaluations of the moisture content predictions by the selected ANNs are described below by comparing the modelling outputs with the experimental measurements.

3.2 Model performance against measured data

Figure 9 shows the predicted daily average moisture content with measured data. Qualitatively, the model captures the seasonal variation, the timing of the peaks and the width of the peaks at the surface with reasonable accuracy. It should be emphasized that, due to measurement limitations, the amplitude of the rain-induced peaks cannot be compared. The final months of the measurement confirm that the model performs well in the absence of precipitation.

The comparison at a depth of 11 mm indicates that the model, at least initially, overestimates the rain-induced peaks, but is able to reproduce the seasonal variation quite well. The limitation regarding the valid moisture range is less problematic in the core of the sample, since the moisture content generally remains within the valid measurement range.

The vertical shaded lines indicate periods of time when one or several weather variables were missing. It can be noted that every instance of missing inputs results in a gap in the output equal to the window of missing data plus an additional 11 days (considering the required lagged inputs for DD modelling). So, the size of these gaps is consistent with L. To reduce the impact of missing data, smaller gaps

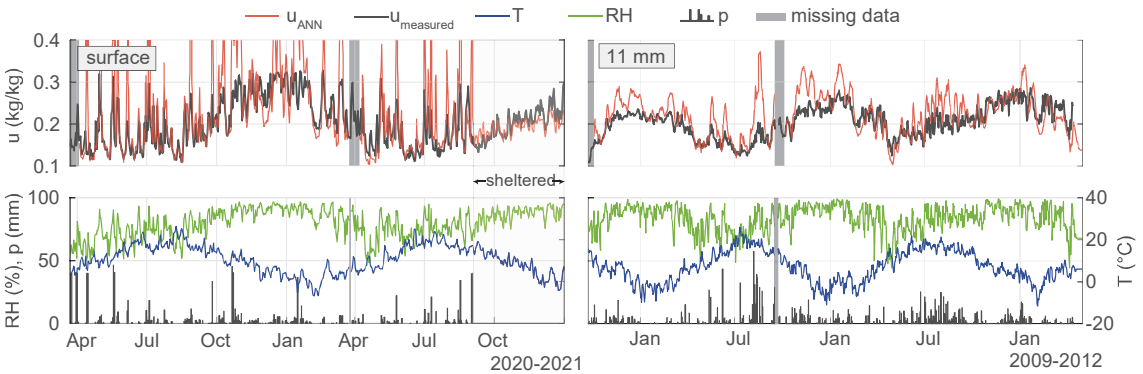

Figure 9: *ANN model compared against measured data (top row) from two different experiments where the moisture content was measured at different depths (surface and 11 mm) together with weather data over the respective periods (bottom row). Shaded vertical lines indicate periods when at least one weather variable is missing.*

https://doi.org/10.52202/069179-0495

can be filled by interpolation of weather prior to the estimations by modelling. Relative humidity and temperature can be interpolated linearly with reasonably low errors since the variation between adjacent days is usually small. Instances of missing precipitation can be substituted by zeros or data from near locations. A single missing rain event will then introduce an unknown degree of uncertainty in the following 11 days of predicted moisture content (if L=11 days) due to the usually high variability of spacetime precipitation. The related error will generally be significant a few days after the missing rain event, and will decrease as the weight of the lagged inputs decrease.

Figure 10 shows the relative time spent above a certain moisture content near the surface. Accordingly, the minimum and maximum measured daily average moisture content are approximately 10% and 32%, respectively, whereas the corresponding modelled values are 10% and >35%. The modelled time spent above a certain threshold remains accurate up until a threshold of u=23%, after which the modelled values increasingly exceed the measurements. As noted in section 2.1.2, this discrepancy can be mainly explained by the nature of the resistance-type measurements. Unless carefully calibrated (see e.g. [18]), measurements based on this technique tend to underestimate the moisture content in the over-hygroscopic moisture range. Consequently, model accuracy cannot be evaluated in the over-hygroscopic region and predicted values should be interpreted and used with caution. The discrepancy already at 23% moisture content is likely related to aggregation of the measurements to daily averages. To clarify, while measurements are relatively accurate up to around 25% moisture content, a daily average of 23% can include sub-daily measurements exceeding 25%. This limitation can be dealt with in durability applications by interpreting any values exceeding 25% as being favourable for fungal decay, and/or by adapting the decay model by reducing the critical moisture-threshold [2].

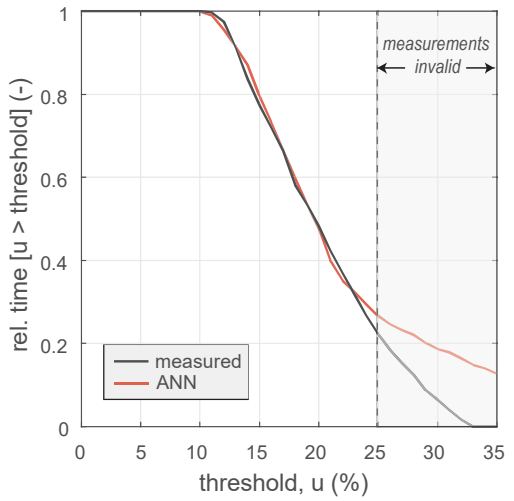

Figure 10: *Measured and modelled relative time spent above a certain moisture content-threshold near the surface.*

4 CONCLUSIONS

Data-driven models can be used to predict moisture content of rain-exposed wood. Contrary to numerical models, data-driven models are efficient and deployable and can thus be integrated into existing digital performance-based service life design frameworks for wood. This will potentially lead to improved and accessible service life prediction of wood.

Using simulated data for model fitting is not ideal, as any errors stemming from the numerical model are transferred to the DD model. In addition, the range of wood species for which the numerical model is valid is limited. On the other hand, when fitting a model to measured data, any uncertainties and limitations (such as the valid measurement range) of the system are instead transferred to the model.

In future work, the model will be used to map decay risk based on data sets with high spatial resolution (on different scales) and longer timespans (multiple years), where numerical models are too computationally expensive.

ACKNOWLEDGEMENT

The second author was funded by Formas (Swedish research council for sustainable development) [2021-02053]. The first and third authors were funded by the ForestValue project WoodLCC which is supported under the umbrella of ERA-NET Cofund ForestValue by the Ministry of Education, Science and Sport (MIZS) - Slovenia; The Ministry of the Environment (YM) - Finland; Research Council of Norway (RCN) - Norway; The Swedish Research Council for Environment, Agricultural Sciences and Spatial Planning (FORMAS), Swedish Energy Agency (SWEA), Swedish Governmental Agency for Innovation Systems (Vinnova) - Sweden; Estonian Ministry of the Environment; Estonian Research Council; Federal Ministry of Food and Agriculture (BMEL) and Agency for Renewable Resources (FNR) - Germany. ForestValue has received funding from the European Union's Horizon 2020 research and innovation programme under grant agreement N° 773324. Thanks to Brendan Nicholas Marais for proofreading the article.

REFERENCES

[1] Thelandersson S., Isaksson T., Suttie E., Frühwald E., Toratti T., Grüll G.: Service life of wood in outdoor above ground applications: Engineering design guideline - Background document. Technical report: TVBK-3061. Lund, Sweden, 2011.

[2] Isaksson T., Brischke C., Thelandersson S.: Development of decay performance models for outdoor timber structures. Materials and Structures, 46:1209–1225, 2013.

[3] Brischke C., Bayerbach R., Rapp A.O.: Decay-influencing factors: A basis for service life prediction of wood and wood-based products. Wood Material Science and Engineering, 1:91–107, 2006.

[4] Brischke C., Meyer L., Bornemann T., Bilstein M., Lauenstein B., Lück J.-M., Wulf C.: Service life of timber components: prognosis based on 3 years high-frequency monitoring. Eurean Journal of Wood and Wood Products, 71(1):79–90, 2013.
[5] Frühwald Hansson E., Brischke C., Meyer L., Isaksson T., Thelandersson S., Kavurmaci D.: Durability of timber outdoor structures: modelling performance and climate impacts. In: World Conference of Timber Engineering, 16-19, 2012.
[6] Niklewski J., Fredriksson M., Isaksson T.: Moisture content prediction of rain-exposed wood: Test and evaluation of a simple numerical model for durability applications. Building and Environment, 97:126–136, 2016.
[7] Awadalla H., El-Dib A., Mohamad M., Reuss M., Hussein H.: Mathematical modelling and experimental verification of wood drying process. Energy Conversion and Management, 45(2):197–207, 2004.
[8] Fortino S., Mirianon F., Toratti T.: A 3D moisture-stress FEM analysis for time dependent problems in timber structures. Mechanics of Time-Dependent Materials, 13:333–356, 2009.
[9] Niklewski J., Van Niekerk P.B., Brischke C., Frühwald Hansson E.: Evaluation of moisture and decay models for a new design framework for decay prediction of wood. Forests, 12(6):721, 2021.
[10] Van Niekerk P.B., Marais B.N., Brischke C., Borges L.M., Kutnik M., Niklewski J., Ansard D., Humar M., Cragg S.M., Militz H.: Mapping the biotic degradation hazard of wood in Europe–biophysical background, engineering applications, and climate change-induced prospects. Holzforschung, 76(2): 188–210, 2022.
[11] Isaksson T., Thelandersson S.: Experimental investigation on the effect of detail design on wood moisture content in outdoor above ground applications. Building and Environment, 59:239–249, 2013.
[12] Niklewski J., van Niekerk P.B., Marais B.N.: The effect of weathering on the surface moisture conditions of Norway spruce under outdoor exposure. Wood Material Science and Engineering, 1–11, 2022.
[13] Hosseini S.H., Hashemi H., Fakheri Fard A., Berndtsson R.: Areal Precipitation Coverage Ratio for Enhanced AI Modelling of Monthly Runoff: A New Satellite Data-Driven Scheme for Semi-Arid Mountainous Climate. Remote Sensing, 14(2): 270, 2022.
[14] Jolliffe I.T.: Principal component analysis for special types of data, Springer, 2002.
[15] Wong S.L., Wan K.K., Lam T.N.: Artificial neural networks for energy analysis of office buildings with daylighting. Applied Energy, 87(2): 551–557, 2010.
[16] Hosseini S.H., Hashemi H., Larsson R., Berndtsson R.: Merging dual-polarization X-band radar network intelligence for improved microscale observation of summer rainfall in south Sweden. Journal of Hydrology, 129090, 2023.
[17] Scheffer T.C.: A climate index for estimating potential for decay in wood structures above ground. Forest Products Journal, 21(10): 25–31, 1971.
[18] Otten K.A., Brischke C., Meyer C.: Material moisture content of wood and cement mortars–Electrical resistance-based measurements in the high ohmic range. Construction and Building Materials, 153: 640–646, 2017.

https://doi.org/10.52202/069179-0495